Response to the review by Isobel R. Lawrence.

Major comments

In order to use this methodology with satellite data from CryoSat-2, ice freeboard (the elevation of the snow/ice interface above the ocean surface) is required. However, it is impossible to retrieve ice freeboard from CryoSat-2 without a-priori knowledge of the snow layer. Since the radar pulse slows down as it travels through the snow, snow depth is required in order to correct for the slower speed of propagation and estimate sea ice freeboard.

To compound the issue, the equation to convert radar freeboard into ice freeboard is incorrectly reported in a number of studies, including that of Kurtz et al. (2014, eq. 16) which describes the CS2 ice freeboard dataset you use in your analysis.

Please see Mallett et al. (2020) for the correct derivation of the equation and details of its misreporting in the literature. The correct equation for sea ice thickness from radar altimetry (assuming full snow penetration) is:

$$H = \left(f_r + h\left(\frac{c}{c_s} - 1\right)\right)\left(\frac{\rho_w}{\rho_w - \rho_i}\right) + h\left(\frac{\rho_s}{\rho_w - \rho_i}\right),$$

where f_r is radar freeboard, as estimated from radar altimeters like CryoSat-2. If this equation cannot be solved by the proposed methodology (I do not believe it can be), then the paper should be restructured to focus on the laser case. The methodology remains valid for use with snow freeboards, and these are available from ICESat and now ICESat-2, so perhaps section 4.3 could be changed to an application to ICESat data. I appreciate that this will require a substantial amount of work, which is why I consider this revision major. However I find this methodology novel and valuable and the results in section 4.2 are encouraging; I would like to reiterate therefore that I think the paper deserves publication subject to this alteration and the following minor revisions:

Thanks for the comment on the fact that the radar algorithm depends on the snow depth, even before retrieving the snow depth. As a matter of fact, another reviewer raised the similar concern, and thus following responses are nearly same.

Recognizing the problems related to the radar altimetry, we modified equations for the model system to handle the radar freeboard as well. The modified model system is delineated in Figure AC2-1 (with slightly changed notations).

Now, the system includes correction terms regarding the wave propagation speed change in the snow layer (F_c), and the displacement of the scattering horizon from the ice surface (F_p) following Kwok and Cunningham (2015) and Armitage and Ridout (2015).

$$F_i = F_r + \left(F_c - F_p\right) \quad \text{(AC2-1)}$$

$$F_c = (\eta_s - 1)\, f h_s \quad \text{(AC2-2)}$$

$$F_p = (1 - f)h_s \quad \text{(AC2-3)}$$

Here, η_s denotes the refractive index of snow layer (η_s=c/c_s) and f denotes the radar penetration factor, respectively. Combining three equations yields the following relationship.

$$F_i = F_r + (f\eta_s - 1)h_s \quad \text{(AC 2-4)}$$

Luckily, we were able to include this issue in the retrieval, by modifying Eqs. (5) and (7) of the manuscript (see below for Eqs. (5) and (7) written with new notation), using Eq. (AC2-4).

Eq. (5): $H_i = \left(\frac{\rho_w}{\rho_w - \rho_i}\right) F_i + \left(\frac{\rho_s}{\rho_w - \rho_i}\right) h_s$

Eq. (7): $H_i = \frac{\rho_w}{\rho_w - \rho_i - \alpha\rho_s} F_i$

It is because Eq. (AC2-4) does not include additional unknowns, for given parameterization and assumption on the radar penetration. We assumed f = 0.84 for CS2 (Armitage and Ridout, 2015). η_s can be parameterized as a function of the snow density, i.e., η_s=$(1+0.51\rho_s)^{1.5}$ (Ulaby et al., 1986). Here we present how the equations were solved.

First, the traditional method for the ice thickness retrieval with the snow depth as input can be written in the following equation by substituting F_i with F_r using Eq. (AC2-4).

$$H_i = \frac{\rho_w}{\rho_w - \rho_i} F_r + \frac{(f\eta_s - 1)\rho_w + \rho_s}{\rho_w - \rho_i} h_s \quad \text{(AC2-5)}$$

Please note that this equation is equivalent to the equation assuming full snow penetration which you presented. Then, substituting h_s with αH_i and rearranging the equation yield the equation for H_i as a function of radar freeboard and α, without snow depth information.

$$H_i = \frac{\rho_w}{\rho_w - \rho_i - \alpha\{(f\eta_s - 1)\rho_w + \rho_s\}} F_r \quad \text{(AC2-6)}$$

Also note that Eq. (AC2-6) becomes equivalent to the equation for the total freeboard if f = 0 (no wave penetration into snow layer).

This new setup requires the data processing chain to be modified as well. Here we describe what changes were made (in Sect. 3.3 and 3.4 of the manuscript). First, CS2-like radar freeboard was derived from OIB total freeboard (F_t^{OIB}) and snow depth (h_s^{OIB}). From Eq. (AC2-4) and the relationship F_i = F_t - h_s, the radar freeboard can be expressed as follows.

$$F_r^{OIB} = F_t^{OIB} - h_s^{OIB} - (f\eta_s - 1)h_s^{OIB} \quad \text{(AC2-7)}$$

Because the main objective of using OIB data is to evaluate the relative performance of the simultaneous retrieval method when the method is applied to CS2 data, the radar penetration factor (f) for OIB data processing is also set to be 0.84 (Artimage and Ridout, 2015). In the data processing chain, h_s^{OIB} is removed if it is smaller than the given uncertainty level of the dataset (~5.7 cm) or it is

larger than the total freeboard F_t^{OIB}.

The CS2 radar freeboard (F_r^{CS2}) was obtained from CS2 ice freeboard dataset. The CS2 ice freeboard data (F_i^{CS2}) distributed by NSIDC (Kurtz et al. 2017) assume that radar scattering horizon locates at snow–ice interface and applies a wave propagation speed correction. However, the correction was made using the MW99 snow depth (h_s^{MW99}) climatology with an erroneous correction form of $h_c = (1-\eta_s^{-1})\, h_s$, instead of the correct correction form of $h_c = (\eta_s - 1)\, h_s$ (Mallet et al. 2020). Thus, at this point, it is straightforward to derive the CS2 radar freeboard by removing the correction term as in the following equation.

$$F_r^{CS2} = F_i^{CS2} - (1 - \eta_s^{-1}) h_s^{MW99} \quad \text{(AC2-8)}$$

Finally, analyses in the first version of the manuscript are conducted again using the radar freeboard rather than using the ice freeboard. This time SIC criteria for α calculation was set to be 95% (original: 98%) for a wider coverage. Figs. AC2-2 to AC2-5 are the reprocessed results which will replace the figures in the manuscript. Despite of these changes, we find little changes in the conclusions we made in the first version of the manuscript. In addition, for more comprehensive information, snow depth comparison results are provided in Fig. AC2-5.

Minor comments

• *I think you need to include an uncertainty budget for your sea ice thickness and snow depth estimates.*

Sensitivity test for our method was conducted and the result will be included as Appendix B in the revised manuscript. In Appendix B, snow depth error caused by α error is presented for different cases of α and freeboard.

• *L30: "However, the radar scattering horizon is often treated as the snow–ice interface". Include Hendricks et al. (2016), Guerreiro et al. (2017), Tilling et al. (2018) as refs here since AWI, LEGOS and CPOM CryoSat-2 ice thickness products all make the same assumption.*

Hendricks et al. (2016), Guerreiro et al. (2017) and Tilling et al. (2018) are now referred in the manuscript.

• *L72: ..."for given densities and freeboard" – (and assuming no snow penetration for laser and full snow penetration for radar)*

We rewrote the sentence as follow:

> "… for given densities, freeboard and assumptions on wave penetration"

• *L138: Could you say how many are discarded based on this criterion, and out of how many total.*

By examining the outputs from the program, we found no outputs discarded by this criterion, therefore, we removed this sentence from the text. Here we provide total number of buoy data obtained from different averaging periods for your information (Table AC2-1, will not be included in the text).

• *L159: Can you provide a reference for the OIB data processing document where the densities are given?*

We now referred Kurtz et al. (2013) in the text.

• *L160: I understand that you keep ice density constant in order to compare with OIB data, but later when comparing with satellite-derived ice thickness should you not then use the densities used in those products for a fair comparison?*

As you mentioned, '*CS2 H*' in Fig 9 of the manuscript should not be same as the CS2 product available from NSIDC. Instead, CS2 ice thickness is reproduced with the same densities and MW99 snow depth for the fair comparison. New figures are given in Fig. AC2-5. We also clarified this data processing in the comparison section.

• *L198: "It was reported…" – By who?*

It was reported by Lee et al. (2018). We clarified this in the manuscript.

• *L200: Where does T_{si} for March come from if the Lee et al. (2018) dataset is only December-February?*

We produced T_{si} for March by applying the same algorithm. We clarified this in the text.

• *L201: "…if data frequency is over 20". Do you mean if 20 days out of the month contain data? Or are you referring to a number of points per grid cell?*

Monthly mean temperature was calculated by gird cell by grid cell and the average was done only for the grid cells where there are more than 20 data available during a month. We clarified this in the manuscript.

• L205: Please could you provide the details and a reference for which OIB dataset you used and where it is available from? i.e. L2, L4, Quicklook?

We utilized L4 dataset for 2011-2013 period, and Quick look dataset for 2014-2015 period. Details on OIB data are now provided in the manuscript. Reference and accessibility information were already included in 'Data availability' section.

> "Five years of OIB data during 2011-2015 period are utilized in this study. Accordingly, OIB level 4 dataset (Kurtz et al., 2015) during 2011-2013 period and Quick look dataset (https://doi.org/10.5067/7Q8HCCWS4I0R, last access: 20 May 2020) during 2014-2015 period are obtained from NSIDC."

• Figure 4: Why do you choose to show us the 7-day averaged plot in Fig.4 when Figure 3 was showing 15-day averaged temperature profiles?

We intended to show results from various averaging period to readers. The results for different averaging period can be found in Figs. 5 and 6 in the text. For your information, same figures for different averaging periods are presented in Fig. AC2-6 (will not be included in the text).

• L235: At the end of this sentence you could refer the reader to the appendix.

Appendix A is now referred at the end of the sentence.

• L244: bias is not near-zero in Fig 4b, it is zero.

Yes, it is zero. The comment is now applied in the text.

• L269: Did you calculate a different alpha for each year, and apply the different alpha to each year of OIB data? Or did you just average all the years together? Please clarify this in the text.

We calculated and applied a different α for each year. It is now clarified in the text.

• L295: Do you get the MW99 for input into Eqs. (4) and (5) from the CS2 data? If so is it monthly grid-averaged? How do you assign each OIB point a snow depth?

Yes, MW99 was obtained from the CS2 dataset. OIB data were reformatted in a 25 km polar stereographic grid by method described in Sect. 3.3 in the manuscript. As OIB data is reformatted into the grid format, it is straightforward to assign the OIB snow depth to the MW99.

One possible concern is that the monthly mean of daily MW99 might differ significantly from the daily MW99, because the MW99 depends on the sea ice type. However, it may not be a critical issue when following points are considered: 1) W99 is already a monthly climatology, 2) ice type distribution would not be changed significantly by the sea ice drift in March because the Arctic Ocean is nearly filled with sea ice and thus the sea ice mobility is reduced.

• L301: "Therefore, if there are decreasing trends in both ice thickness and snow depth, the decreasing trend of ice thickness estimated from the constant snow depth will be diminished in radar, while being amplified in lidar" – This sentence seems overcomplicated. To me, all that the bottom two plots of Figure 7 demonstrate is that MW99 snow depth is larger than OIB snow depth. For the laser case, this means that using W99 causes ice thickness to be underestimated compared to H(OIB), and for the radar case using W99 results in ice thicknesses that are too thick compared to OIB. Perhaps you could plot MW99 against h(OIB) to clarify this? The retrieval of sea ice thickness from ICESat has not traditionally used the Warren climatology- see Kwok and Cunningham (2008) and Petty et al. (2020). Therefore I don't think it's justified to call this 'ICESat-like thickness' since you are not using the same snow depth product that they do.

Yes, what you mentioned is the appropriate interpretation of Fig. 7; MW99 is larger than OIB snow depth. This can be verified by Fig. S1 (will be included as a supplementary figure in the text). However, we attempted to address a possible unintended result of 'diverging direction in errors in ice thickness retrieval, when the same snow depth error is applied to two different satellite altimetry measurements'. We modified this paragraph to deliver such message.

> "The negative bias of ICESat-like thickness and positive bias of CS2-like thickness compared to H_i^{OIB} demonstrate that h_s^{MW99} is greater than h_s^{OIB} (as shown in Fig. S1), according to Eqs. (4) and (5). In other words, the sensitivity of ice thickness diverges for two different types of altimeter to the same snow depth error. Therefore, …"

Regarding the naming issue, we are not referring existing products when we call ICESat-like and CS2-like thickness. Those are explicitly defined in the text:

> "In doing so, OIB-measured total freeboard and ice freeboard are converted into ice thickness using MW99 as input to solve Eqs. (4) and (5). These two ice thickness retrievals are referred to as ICESat-like thickness and CS2-like thickness, respectively"

Besides, there is an ice thickness dataset from ICESat total freeboard distributed by NSIDC (Yi and Zwally, 2009; doi: 10.5067/SXJVJ3A2XIZT) which uses MW99. However, we think that the expression "current practices of retrieving sea ice thickness" might confuse readers. Therefore, we will replace such expression with "MW99 method" for clarity.

Typos / Grammar

• *L128: "Therefore, the interface searching algorithm…" -> "Therefore, an interface searching algorithm…"*

• *L165: "Sea ice thicknesses converted from MW99 using Eqs. (4) and (5) are also compared to examine how simultaneous retrievals…" -> "Sea ice thicknesses are also calculated from Eqs. (4) and (5), using MW99 as snow depth, to examine how simultaneous retrievals…"*

• *L194: "This reformatted AASTI-v2 data are called…" -> "This reformatted AASTI-v2 dataset is called…"*

• *L293: "Examining how the current practices of retrieving the sea ice thickness through ICESat and CS2 measurements are compared with the simultaneous retrievals is of interest" -> "We now examine how the current practises of retrieving sea ice thickness from ICESat and CS2 measurements compare with our method."*

• *L294: "In doing so, OIB-measured…" -> "To do so, OIB-measured…"*

• *L297: "Apparently, ICESat-like thickness tends…." -> "According to our analysis, ICESat-like thickness tends…."*

• *L416: "…which are hard to be quantified explicitly." -> "…which are hard to quantify explicitly."*

All comments are applied in the manuscript.

References

Armitage, T. W. K., and Ridout, A. L.: Arctic sea ice freeboard from AltiKa and comparison with CryoSat-2 and Operation IceBridge, Geophys. Res. Lett., 42, 6724–6731, doi: 10.1002/2015GL064823, 2015.

Guerreiro, K., Fleury, S., Zakharova, E., Kouraev, A., Rémy, F., and Maisongrande, P.: Comparison of CryoSat-2 and ENVISAT radar freeboard over Arctic sea ice: toward an improved Envisat freeboard retrieval, Cryosphere, 11, 2059–2073, doi: 10.5194/tc-11-2059-2017, 2017.

Hendricks, S., Ricker, R., and Helm, V.: User Guide – AWI CryoSat-2 sea Ice thickness data product (v1.2), doi: 10013/epic.48201, 2016.

Kurtz, N. T., Farrell, S. L., Studinger, M., Galin, N., Harbeck, J. P., Lindsay, R., Onana, V. D., Panzer, B., and Sonntag, J. G.: Sea ice thickness, freeboard, and snow depth products from Operation IceBridge airborne data, Cryosphere, 7, 1035–1056., doi: 10.5194/tc-7-1035-2013, 2013.

Kurtz, N. T., Galin, N., and Studinger, M.: An improved CryoSat-2 sea ice freeboard retrieval algorithm through the use of waveform fitting, Cryosphere, 8, 1217–1237, doi: 10.5194/tc-8-1217-2014, 2014.

Kurtz, N., M. Studinger, J. Harbeck, V. Onana, and D. Yi.: IceBridge L4 Sea Ice Freeboard, Snow Depth, and Thickness, Version 1, National Snow and Ice Data Center, doi: 10.5067/G519SHCKWQV6, 2015.

Kwok, R., and Cunningham, G. F.: Variability of Arctic sea ice thickness and volume from CryoSat-2, Phil. Trans. R. Soc. A, 373(2045), 20140157, doi: 10.1098/rsta.2014.0157, 2015.

Lee, S.-M., Sohn, B.-J., and Kummerow, C. D.: Long-term Arctic snow/ice interface temperature from special sensor for Microwave imager measurements, Remote Sens., 10(11), 1795, doi: 10.3390/rs10111795, 2018.

Mallett, R. D. C., Lawrence, I. R., Stroeve, J. C., Landy, J. C., and Tsamados, M.: Brief communication: Conventional assumptions involving the speed of radar waves in snow introduce systematic underestimates to sea ice thickness and seasonal growth rate estimates, The Cryosphere, 14, 251-260, doi: 10.5194/tc-14-251-2020, 2020.

Tilling, R. L., Ridout, A., and Shepherd, A.: Estimating Arctic sea ice thickness and volume using CryoSat-2 radar altimeter data, Adv. Space Res., 62, 1203–1225, doi: 10.1016/j.asr.2017.10.051, 2018.

Ulaby, F. T., Moore, R. K., and Fung, A. K.: Microwave remotesensing: Active and passive, Volume 3-From theory to applications, 1986.

Yi, D., and H. J. Zwally: Arctic Sea Ice Freeboard and Thickness, Version 1, National Snow and Ice Data Center, doi: 10.5067/SXJVJ3A2XIZ, 2009.

Table AC2-1. Number of outputs obtained from the interface searching algorithm

Averaging period	# of obtained outputs
1 day	542
7 days	97
15 days	59
30 days	36

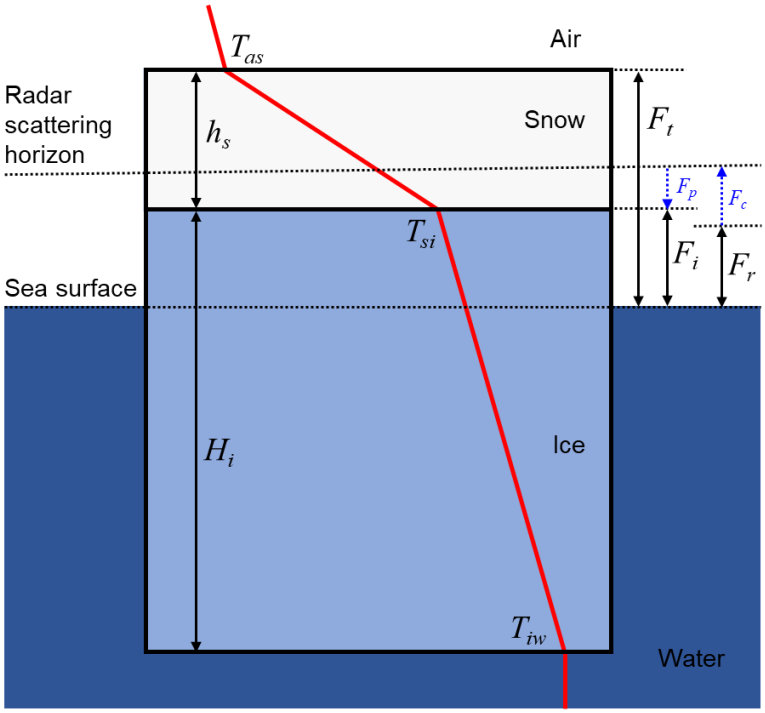

Figure AC2-1. Schematic diagram of a typical snow–ice system during the winter. Snow depth (h_s), ice thickness (H_i), total freeboard (F_t), radar freeboard (F_r), and ice freeboard (F_i) are indicated. Correction terms regarding the wave propagation speed change in snow layer (F_c) and the displacement of the scattering horizon from the ice surface (F_p) are indicated by blue arrows. Red line denotes a typical temperature profile with air–snow interface temperature (T_{as}), snow–ice interface temperature (T_{si}) and ice–water interface temperature (T_{iw}). *In the text, change was also made on the notation for the bulk densities of materials (ρ_i: density of sea ice, ρ_s: density of snow, ρ_w: density of sea water).*

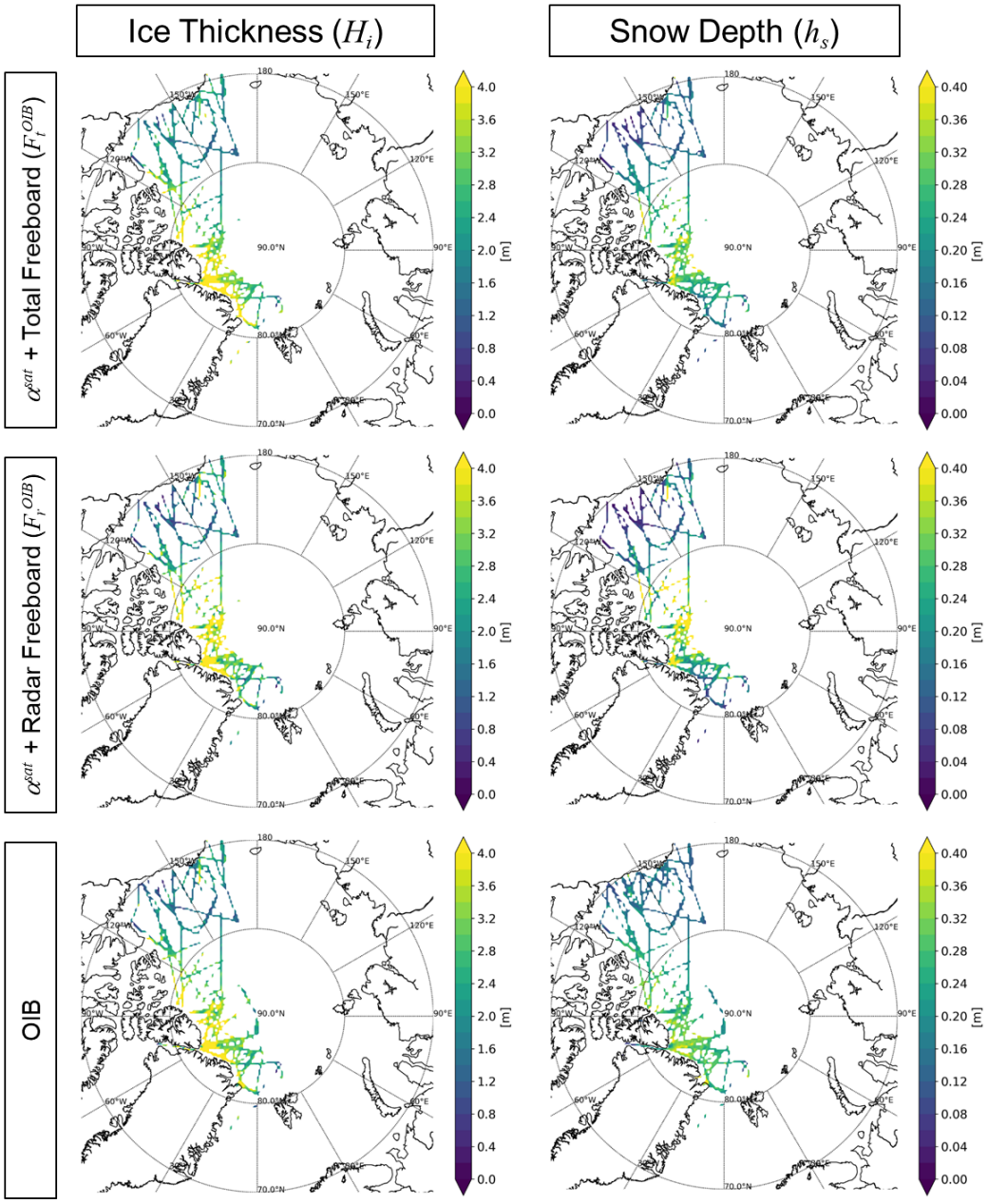

Figure AC2-2. Simultaneously retrieved ice thickness and snow depth from OIB total/radar freeboard in March of the 2011–2015 period. Corresponding OIB products are at the bottom.

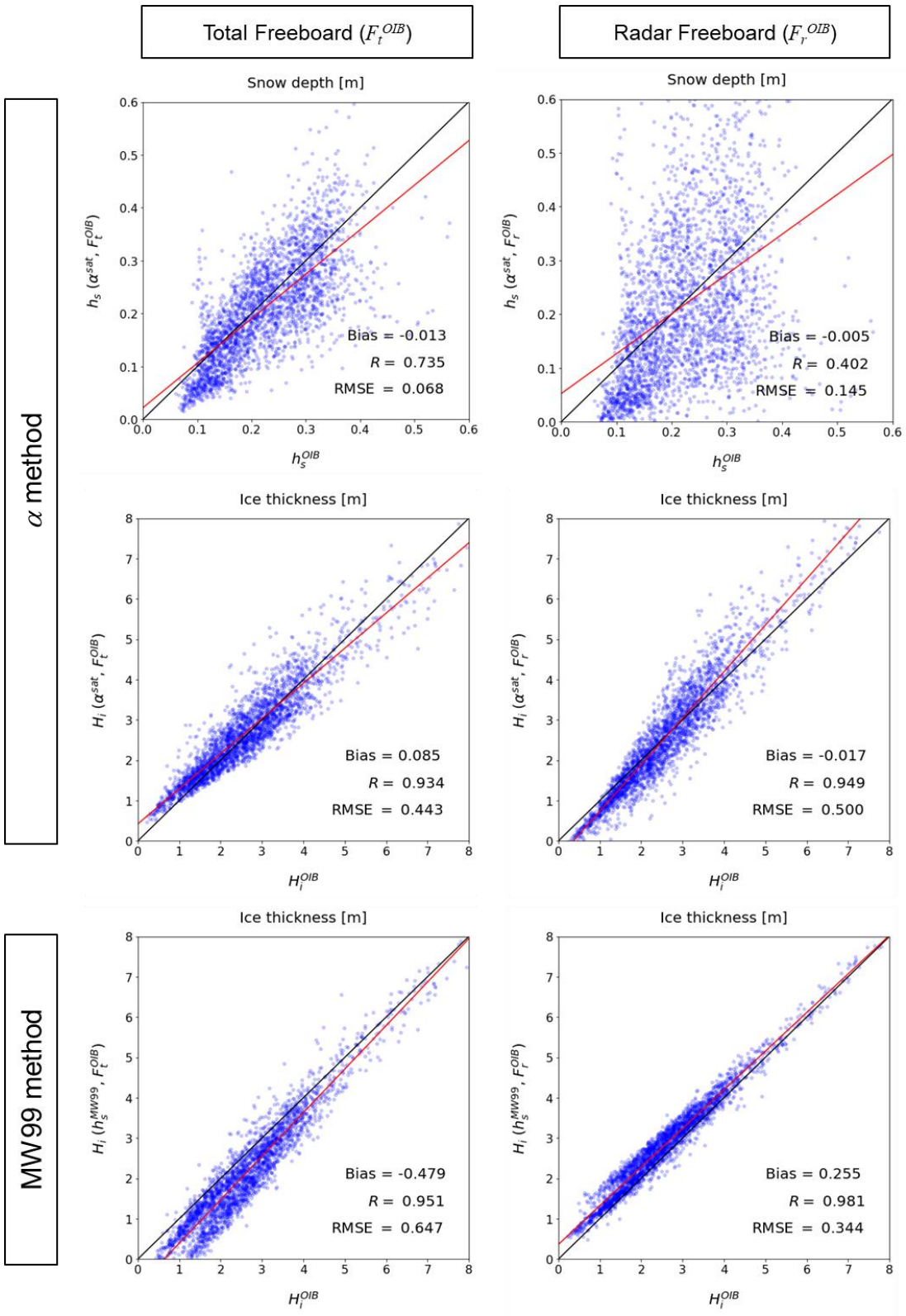

Figure AC2-3. Scatter plots between OIB products and the simultaneously retrieved snow depth and ice thickness from OIB total/radar freeboards during the March 2011–2015 period. Corresponding ice thicknesses estimated from MW99 snow depth are in the third row. The red lines are linear regression lines.

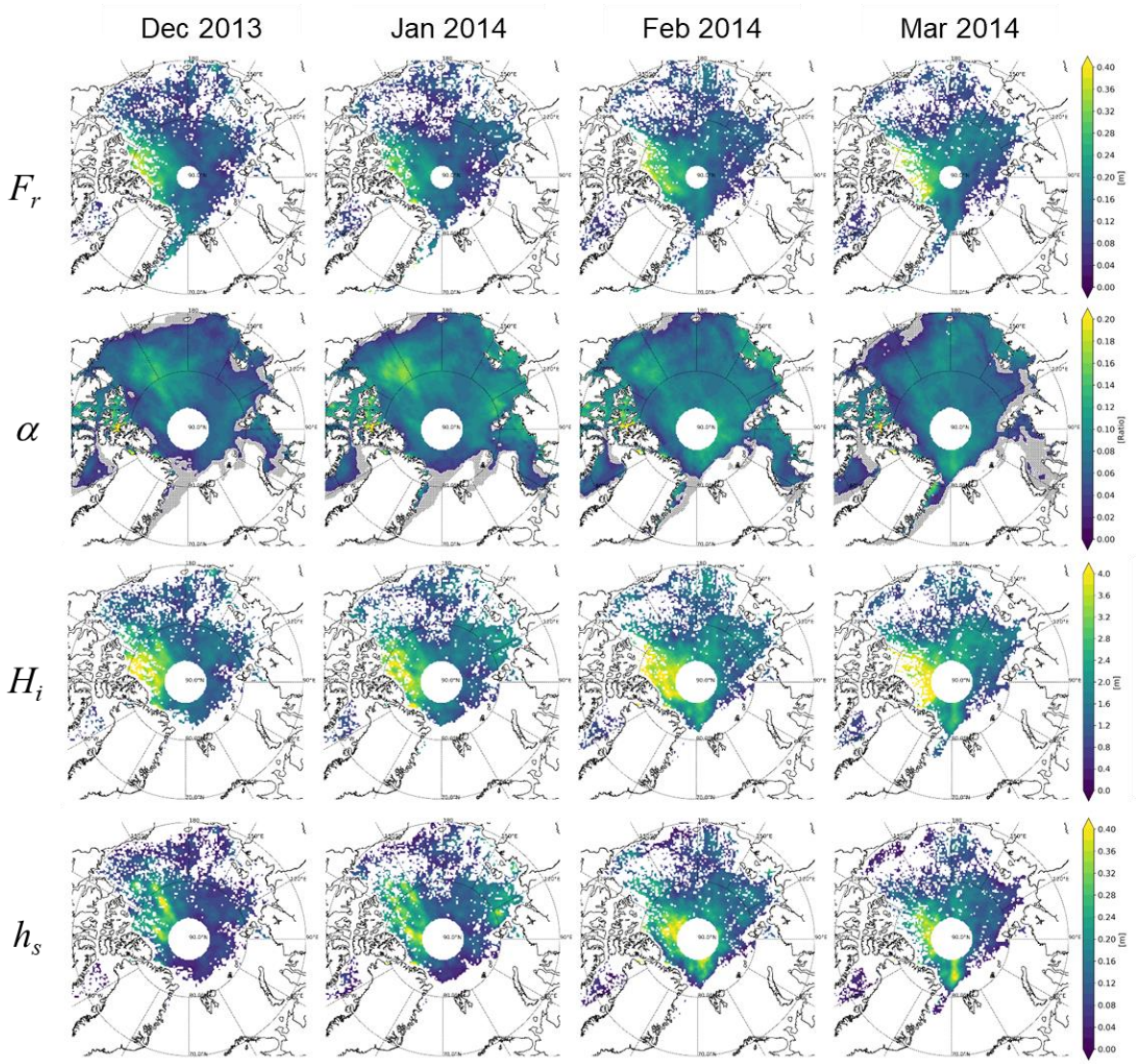

Figure AC2-4. Geographical distributions of observed CS2 radar freeboard (F_r) and estimated snow–ice thickness ratio (α), ice thickness (H_i), and snow depth (h_s) from December 2013 to March 2014. Grey area in the second row denote where α retrieval is failed because T_{as} is warmer than T_{as}.

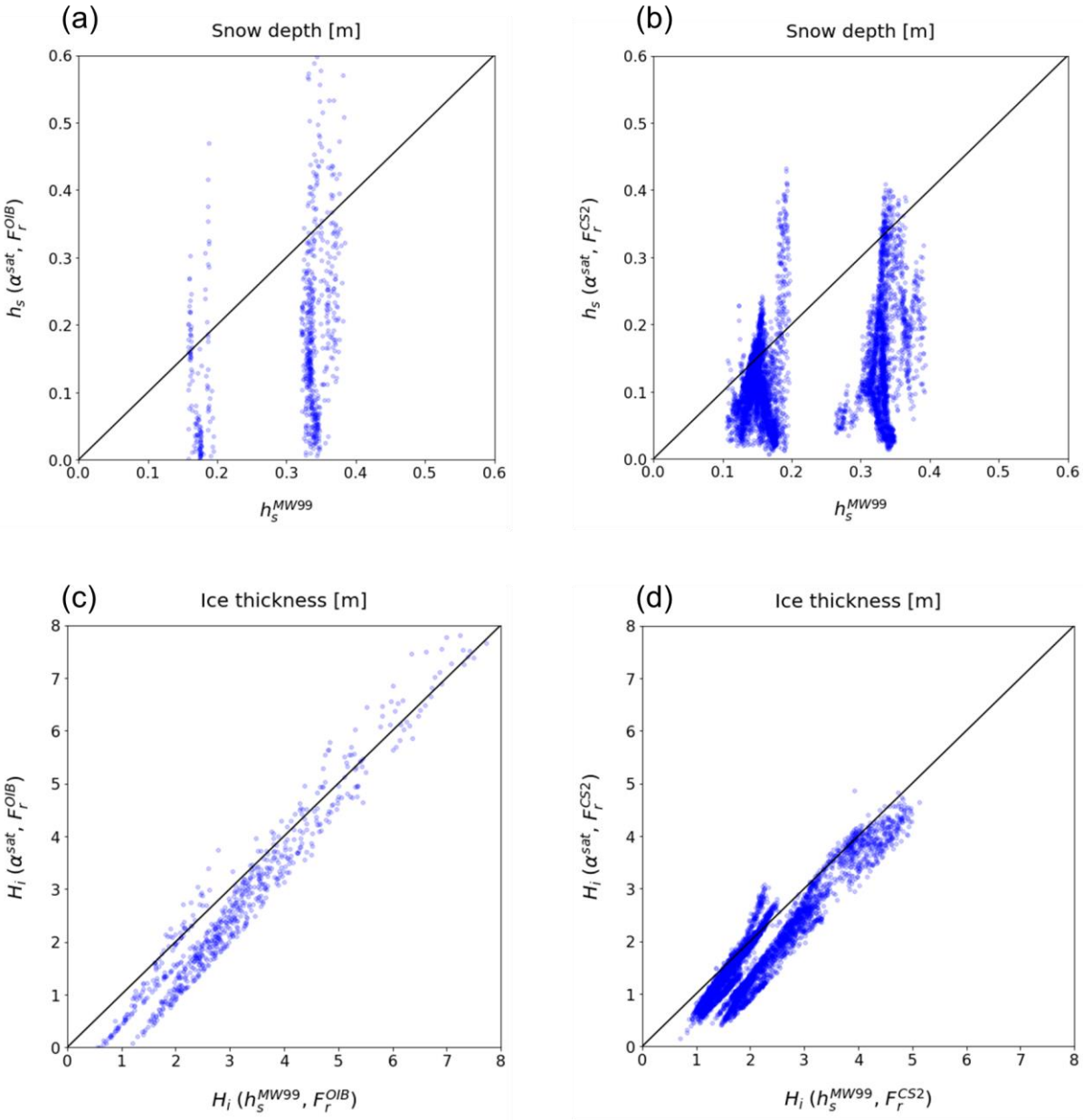

Figure AC2-5. Comparison of simultaneous retrieved snow depth and ice thickness to those from MW99 method. (a) Snow depth from OIB radar freeboard, (b) snow depth from CS2 radar freeboard, (c) ice thickness from OIB radar freeboard, and (d) ice thickness from CS2 radar freeboard.

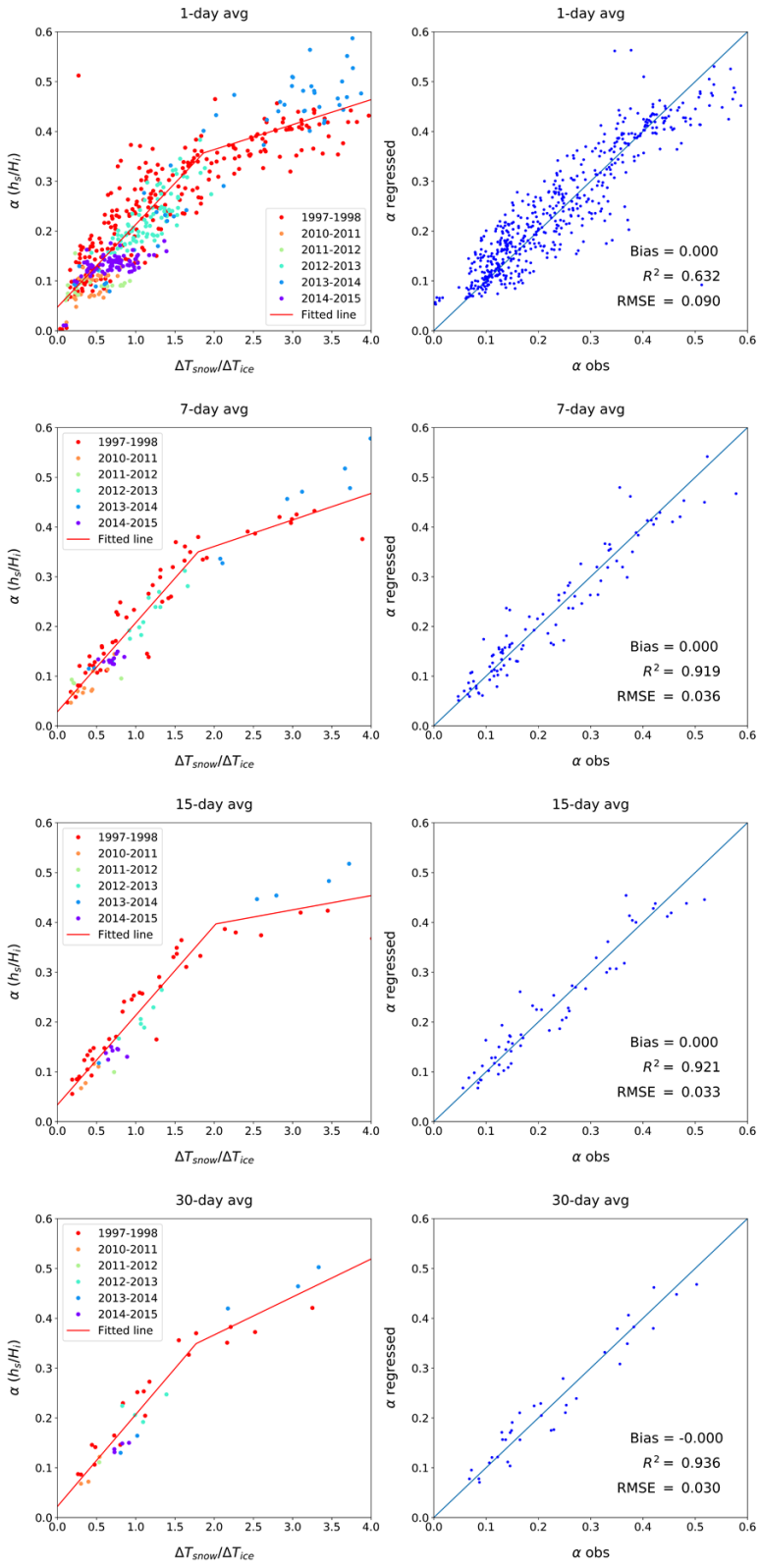

Figure AC2-6. (Left column) Scatterplots of the temperature difference ratio of the snow and ice layer ($\Delta T_{snow}/\Delta T_{ice}$) and the snow–ice thickness ratio (α) for averaging period of 1,7,15 and 30 days. Color denotes collected year of buoy data. The red lines are the regression lines (defined in Eq. (8) in the text). (Right column) The corresponding scatter plot of observed and regressed α.

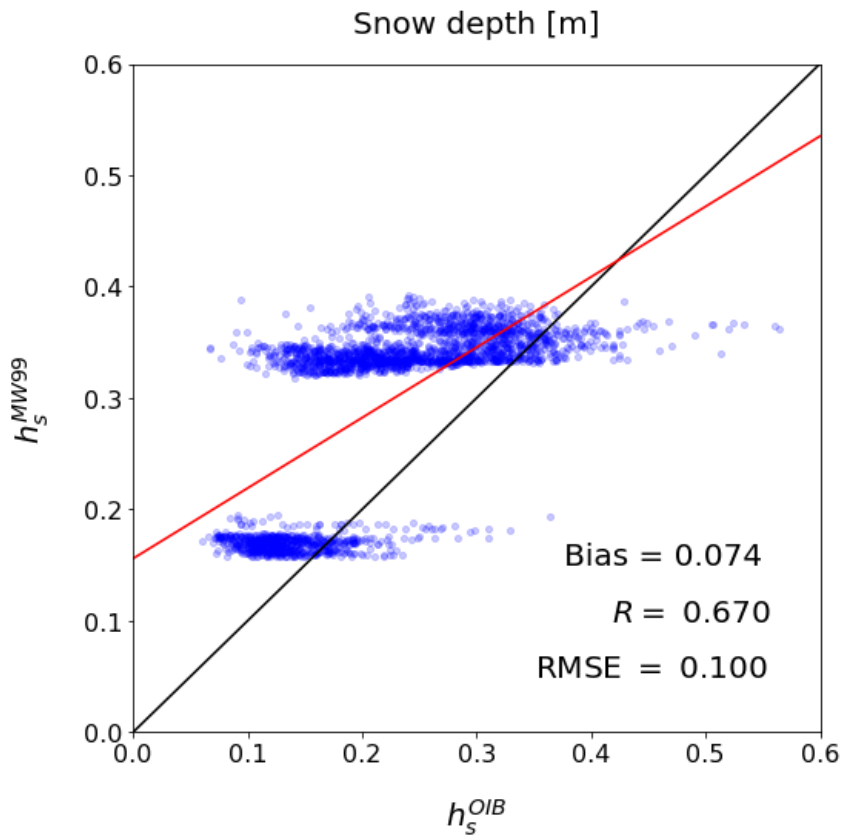

Figure S1. Comparison between OIB snow depth and MW99 snow depth during March of 2011-2015 period.

Appendix B. Sensitivity test for the proposed method

Here we present results of the sensitivity test of showing how the snow depth and ice thickness retrieval results are dependent on the uncertainties in α. To do so, the uncertainty in the snow depth (Δh_s) due to the α error (i.e. $\Delta\alpha$) and associated ice thickness error (ΔH_i) are estimated. From this sensitivity test, we expect to understand why the simultaneous method for the radar freeboard shows more scattered features than those from the method for the lidar total freeboard.

First, Δh_s is defined by the difference of retrieved h_s between with error ($\alpha+\Delta\alpha$) and without error (α).

$$\Delta h_s = \begin{cases} h_s(\alpha+\Delta\alpha, F_t) - h_s(\alpha, F_t) & (\text{using } F_t) \\ h_s(\alpha+\Delta\alpha, F_r) - h_s(\alpha, F_r) & (\text{using } F_r) \end{cases} \quad \text{(B1)}$$

Then, Δh_s can be converted to the error in the ice thickness (ΔH_i) using the following equation derived from Eq. (AC2-5).

$$\Delta H_i = \frac{(f\eta_s - 1)\rho_w + \rho_s}{\rho_w - \rho_i}\Delta h_s = \begin{cases} -6.46\Delta h_s & (\text{using } F_t) \\ 3.44\Delta h_s & (\text{using } F_r) \end{cases} \quad \text{(B2)}$$

Because h_s is a combination of freeboard and α, as in Eq. (AC2-6), we only examine the uncertainty with some representative sea ice types. Here physical states for thicker ice (type A), moderate ice (type B) and thinner ice (type C) are chosen, which are summarized in Table B1. Those typical values are for three types are shown over the scatterplots of OIB-based (α vs. F_t) and of satellite-based (α vs. F_r) – Fig. B1. It is shown that the majority of data points are located around type B, followed by type A. There seem a very small portion of total samples showing values around the type C.

With $\Delta\alpha = \pm 0.03$, which is an RMSE range of the α-prediction equation, Δh_s and ΔH_i are estimated for the three ice types. Results summarized in Table B2 show that $|\Delta h_s|$ is within 5 cm and it tends to decrease as the ice becomes thinner, when the current method is applied to the total freeboard. On the other hand, $|\Delta h_s|$ shows more sensitive behavior for the same $\Delta\alpha$ when the radar freeboard is used for the retrieval. Especially, the sensitivity of type C is the greatest. This is because the denominator of Eq (AC2-6) becomes smaller when α approaches to α_{crit}, resulting in unstable solution. For the ice thickness, $|\Delta H_i|$ is smaller when the total freeboard is used since ΔH_i is proportional to Δh_s. However, the gap between the results from two freeboards has narrowed because H_i from the total freeboard is more sensitive than the radar freeboard to Δh_s, according to Eq. (B2). Sensitivity characteristics shown here are consistent with analysis results given in Sect 4.2. Because there is a much small number of data points belonging to the type C, at least in the data used for this study, the overall sensitivity would likely be in between the B and A types.

It is also of importance to ask to what degree of retrievals is successfully yielded. In this study, cases showing $T_{as} > T_{si}$ or retrieved $\alpha \geq \alpha_{crit}$ are considered to be failures. Statistics on success/fail ratio of α retrieval for December–March of 2011–2015 period are provided in Table B3. Overall, the success ratio was over 82% in December–February, while it was reduced to ~74% in March. Most of failures appear due to the temperature inversion (i.e. $T_{as} > T_{si}$). Regions showing such a temperature inversion are shown with grey shades in the α-distributions of Fig. AC2-4. The grey areas are generally found around the marginal ice zones and in the east of Greenland.

On the other hand, there were near zero failure (0.02% of total pixels) for retrieved $\alpha \geq \alpha_{crit}$. This near zero failure implies that almost all calculated α meet the satisfactory condition after the removal of cases showing temperature inversion. It may be concluded that calculated α appears to be physically reasonable (i.e. $\alpha < \alpha_{crit}$) as long as presumed thermodynamic conditions are met.

Table B1. Physical state of representative cases of point A, B and C.

Type	H_i **[m]**	h_s **[m]**	α	F_t **[m]**	F_r **[m]**
A	3.961	0.332	0.084	0.65	0.30
B	1.646	0.123	0.075	0.26	0.13
C	0.616	0.152	0.246	0.17	0.01

Table B2. Error of snow depth (Δh_s) and ice thickness (ΔH_i) for snow depth to ice thickness ratio error ($\Delta\alpha$) of ±0.03.

	Total freeboard method		Radar freeboard method	
$\Delta\alpha$	-0.03	0.03	-0.03	0.03
		Δh_s (cm)		
A	-4.070	3.161	-14.59	19.54
B	-1.913	1.471	-5.840	7.730
C	-0.045	0.039	-7.230	37.62
		ΔH_i (m)		
A	0.263	-0.204	-0.502	0.672
B	0.124	-0.095	-0.201	0.266
C	0.003	-0.003	-0.249	1.294

Table B3. Statistics of success/fail ratio α retrieval for 2011-2015 winter.

Year Month	Total Pixels (SIC > 95%)	Success		Fail ($T_{as} > T_{si}$)		Fail ($\alpha > \alpha_{crit}$)	
2010 12	13879	12080	(87.04%)	1799	(12.96%)	0	(0.00%)
2011 01	16246	14004	(86.20%)	2242	(13.80%)	0	(0.00%)
2011 02	17986	14779	(82.17%)	3206	(17.82%)	1	(0.01%)
2011 03	17610	12871	(73.09%)	4738	(26.91%)	1	(0.01%)
2011 12	13915	11405	(81.96%)	2510	(18.04%)	0	(0.00%)
2012 01	16812	13765	(81.88%)	3047	(18.12%)	0	(0.00%)
2012 02	17528	14131	(80.62%)	3397	(19.38%)	0	(0.00%)
2012 03	18741	13586	(72.49%)	5155	(27.51%)	0	(0.00%)
2012 12	14059	11144	(79.27%)	2915	(20.73%)	0	(0.00%)
2013 01	16413	13510	(82.31%)	2903	(17.69%)	0	(0.00%)
2013 02	18640	15526	(83.29%)	3114	(16.71%)	0	(0.00%)
2013 03	19078	14134	(74.09%)	4944	(25.91%)	0	(0.00%)
2013 12	14515	12071	(83.16%)	2444	(16.84%)	0	(0.00%)
2014 01	16880	14201	(84.13%)	2678	(15.86%)	1	(0.01%)
2014 02	16987	14731	(86.72%)	2247	(13.23%)	9	(0.05%)
2014 03	17699	13300	(75.15%)	4391	(24.81%)	8	(0.05%)
2014 12	14071	11119	(79.02%)	2952	(20.98%)	0	(0.00%)
2015 01	17008	15095	(88.75%)	1913	(11.25%)	0	(0.00%)
2015 02	18076	15907	(88.00%)	2169	(12.00%)	0	(0.00%)
2015 03	17618	14042	(79.70%)	3576	(20.30%)	0	(0.00%)
December	70439	57819	(82.08%)	12620	(17.92%)	0	(0.00%)
January	83359	70575	(84.66%)	12783	(15.33%)	1	(0.00%)
February	89217	75074	(84.15%)	14133	(15.84%)	10	(0.01%)
March	90746	67933	(74.86%)	22804	(25.13%)	9	(0.01%)

α_{crit}=0.291 for ρ_s=320 kg m^{-3}, ρ_i=915 kg m^{-3}, ρ_w=1024 kg m^{-3}, and f=0.84.

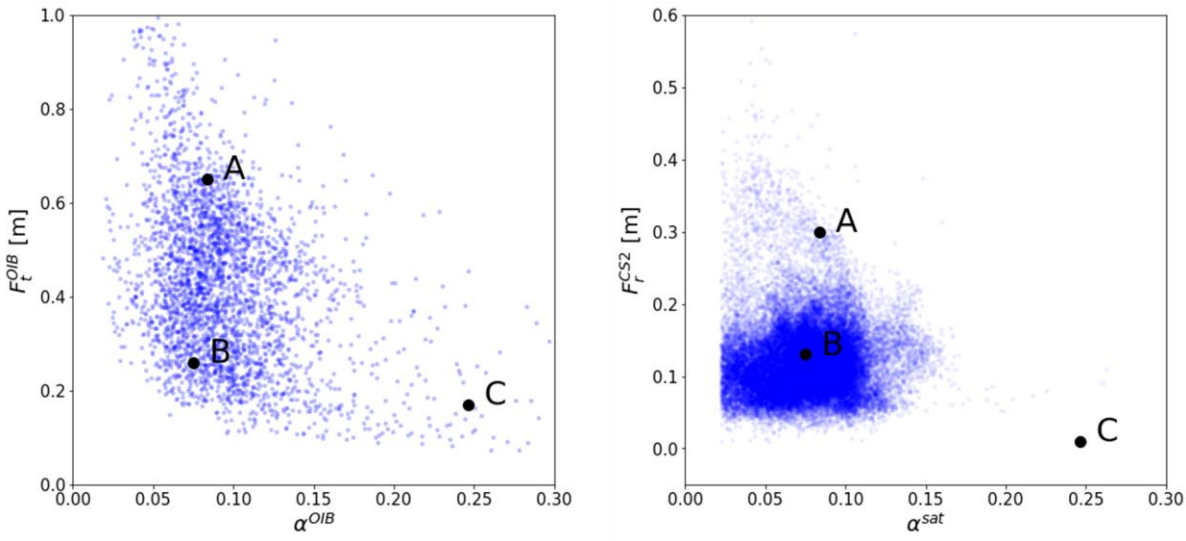

Figure B1. Location of physical state of representative types (A, B, C) on the freeboard-thickness ratio space. Blue dots are from (left) OIB data and (right) retrieved thickness ratio and CS2 radar freeboard.